Composites Part A 125 (2019) 105571

Contents lists available at ScienceDirect

Composites Part A

journal homepage: www.elsevier.com/locate/compositesa

Book reviews

Magnetic programming of 4D printed shape memory composite structures

Fenghua Zhang[a], Linlin Wang[a], Zhichao Zheng[a], Yanju Liu[b], Jinsong Leng[a,*]

[a] National Key Laboratory of Science and Technology On Advanced Composites in Special Enviroments, Harbin Institute of Technology (HIT), No.2 Yikuang Street, P.O. Box 3011, Harbin 150080, People's Republic of China

[b] Department of Astronautical Science and Mechanics, Harbin Institute of Technology (HIT), No. 92 West Dazhi Street, P.O. Box 301, Harbin 150001, People's Republic of China

ARTICLE INFO

Keywords:
Shape memory polymers
4D printing
Magnetic field actuation
Complex structures

ABSTRACT

4D printed shape memory polymers and their composites are currently a highly topical research area. The potential applications for 4D printed smart materials are wide-reaching, with particular promise for personalized medicine. In this work, we 4D printed various structures made of biocompatible and biodegradable polylactic acid (PLA) and PLA/Fe_3O_4 composite filaments. The shape memory behaviors of the 4D printed structures triggered by magnetic field were investigated. The printed structures can return to their original shapes with a high speed in just a few seconds. Moreover, the structures like bone tissues printed by PLA/Fe_3O_4 composites filaments with 15% Fe_3O_4 were actuated by magnetic field at 27.5 kHz. During the shape recovery process, surface temperature of the printed structures is uniform and around 40 °C. This physiologically relevant operating temperature range is a highly attractive feature for potential healthcare and biomedical applications.

1. Introduction

4D printing technology is a rapidly emerging new area of research that refers to the additive manufacturing of shape memory structures [1–3]. 4D printed structures have wide range of potential applications in aerospace [4], flexible electronic devices [5], photo responsive device [6], and biomedical science [7–10]. Compared to traditional additive manufacturing technologies [11], 4D printing is an attractive approach to integrate smart materials with structure manufacturing [12]. The advantages of 4D printing is that the printed structures show shape changing behaviors depending on time [13]. The smart materials for 4D printing include shape memory polymers (SMPs) [14], shape memory alloys (SMAs)[15], shape memory hydrogels [16],and liquid crystal elastomers [17]. Among these materials, SMPs have attracted increasing attention in recent few years due to the low cost, easy processing, and large, reversible deformation capability [18–21].4D printed structures can return to the original shape in response to one or multiple external stimuli, including heat, light, water, electrical and magnetic fields.

A group of researchers at MIT first reported 4D printing technology combining SMPs with 3D printing in 2013 [22]. Later, increasing numbers of researchers are focusing on the subject to obtain suitable SMP structures using additive manufacturing technology, thereby further expanding the range of application areas for smart polymers [23–25].At present, 4D printing is a highly specific technique, in which different printing machines and methods require specific optimization of material properties. Suitable printing methods include PolyJet [26], digital light processing (DLP) [27], direct-writing (DW) [28], and fused deposition modeling (FDM) [29,30]. Notably, Ge et al. printed SMPs with origami structures shown the self-organization function [26]. In addition, Huang et al. fabricated the UV cured SMPs and 4D printed complex structures by DLP [27].Furthermore, Wei et al. used DW printer to fabricate polylactic acid (PLA) nanocomposite micro-scaffolds [28]. More recently, Zhang et al. printed a textile tube functional composite by FDM and demonstrated the shape recovery force and behaviors [29].

In particular, 4D printed SMPs and structures play a significant role in biomedical science, due to the requirements of personalized implant devices and medicine [31]. Potential 4D structures include cell culture [32], tissue engineering scaffolds [27,33,34], tracheal stents [20], drug carriers [35],and implant devices [36,37]. Due to the shape-changing and recovery properties of SMPs, 4D printed implant devices have clear advantages in clinical operations, including biodegradability, low invasive and remote intervention approach, and non-contact control [27]. Compared to the reported work, it is significant and highly desirable to develop a class of smart composite filaments with multiple functions and remote actuation for biomedical engineering.

Herein, we fabricated pure PLA filaments and magnetic PLA/Fe_3O_4

* Corresponding author.
E-mail address: lengjs@hit.edu.cn (J. Leng).

https://doi.org/10.1016/j.compositesa.2019.105571
Received 18 April 2019; Received in revised form 1 August 2019; Accepted 3 August 2019
Available online 03 August 2019
1359-835X/

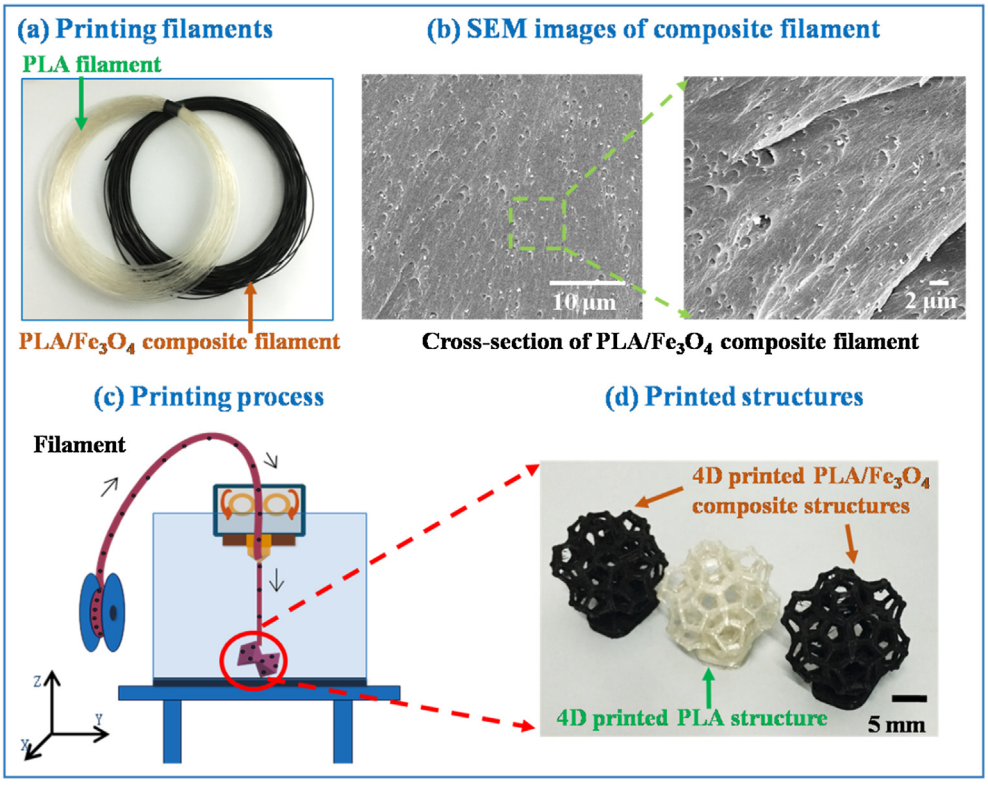

Fig. 1. 4D printing: (a) PLA and PLA/Fe_3O_4 printing filaments; (b) SEM images of composite filament; (c) printing process; (d) printed structures. (For interpretation of the references to colour in this figure legend, the reader is referred to the web version of this article.)

composite filaments with shape memory effect of remotely controlled actuation. The properties of the filaments were analyzed using differential scanning calorimeter (DSC), thermogravimetric analysis (TGA), Fourier transform infrared spectroscopy (FT-IR), dynamic mechanical analyzer (DMA) and scanning electron microscopy (SEM). Moreover, the filaments were printed into different structures by fused deposition modeling (FDM). The shape changing behaviors and thermal distribution of 4D printed structures were investigated. Furthermore, we 4D printed composite shape memory structures in the shape of spinal bones and demonstrated their shape deployable process under magnetic field.

2. Experimental section

2.1. Fabrication of filaments

Poly-lactic acid (PLA) based SMP filaments from Harbin Institute of Technology (HIT) [29] and Fe_3O_4 particles were purchased from Aladdin Chemistry Co., Ltd., Shanghai, China and used without any pretreatment. PLA was dissolved in $CHCl_2$ solvent at room temperature, Fe_3O_4 particles were added in PLA solution to make the Fe_3O_4/PLA composite with mass fractions of 10%, 15% and 20%. PLA/Fe_3O_4 composite filaments were fabricated by a double screw extruder (CTE 20, Coperion Nanjing Machinery Co., Ltd) with six temperature controllers for optimal mixing of composites. The extruder was firstly heated with temperatures at different sections set as 175 °C, 175 °C, 175 °C, 175 °C, 175 °C, and 180 °C, respectively. Then raw materials were added to the feeder. After the six heat sections, the materials went through a cooling system and a tracking device to form the filaments. The diameter of the filament was controlled at 1.75 ± 0.5 mm.

2.2. 4D printing of composite structures

The filaments were added into the FDM printer (Colido 1.0 Plus, Tianwei Co., Ltd). The printing temperature was set to 190 °C. The diameter of the printer head was 0.5 mm. The printing speed was 2 mm/min.

2.3. Characterization

Differential scanning calorimeter (DSC, DSC 1 STAR System, METTLER TOLEDO) measurements were performed under nitrogen. The samples were heated from 0 to 250 °C and then cooled down to 0 °C at a rate of 10 °C/min. Thermogravimetric analysis (TGA) (TGA/DSC 1 STAR System, METTLER TOLEDO) was carried out. The samples were heated from 25 to 500 °C at a rate of 10 °C/min in nitrogen atmosphere. Fourier transform infrared spectroscopy (FT-IR) of the samples was carried out using PerkinElmer FI-TR Spectrometer Spectrum Two following the attenuated total reflectance method. The spectra were obtained under ambient conditions at a resolution of 2 cm^{-1} and 40 scans for each characterization. The mechanical performance was tested with a dynamic mechanical analyzer (DMA, TA) at a constant frequency of 1 Hz from 25 °C to 150 °C at a heating rate of 10 °C/min. The morphology of PLA/Fe_3O_4 composite filament was observed by FEI Nova Nano SEM FEG. Infrared thermographic images were captured using an infrared camera (JENOPTIK InfraTec) to evaluate the temperature distribution of the 4D printed complex structures during the shape recovery process. All solid state induction heating equipment (HR-BP-30, Zhengzhou Huarui Electromagnetic Technology Co., Ltd, China) was used for measuring shape recovery behavior of the printed structures. Power supply for the equipment is alternating current (AC) 50 Hz, 380 V. The oscillation frequency of the circuit is from 27.5 to 47.5 kHz. Alternating current rectificated into direct current and direct voltage is about 440 V.

2.4. Magnetic field induced shape memory behaviors

The shape memory behaviors of 4D printed structures were investigated by magnetic field at 27.5–47.5 kHz.

Table 1
TGA results of PLA/Fe_3O_4 composite filaments with different contents of Fe_3O_4 particles.

Samples	Pure PLA	PLA/Fe_3O_4 10%	PLA/Fe_3O_4 15%	PLA/Fe_3O_4 20%
TD (°C)	161.54	314.42	311.84	302.35
T_{dmax} (°C)	388.24	362.79	354.11	349.10
Residual content	0%	10.53%	14.78%	20.45%

The shape memory behaviors were examined by a bending test using rectangular strip specimens as the permanent shape. The shape fixity ratio (R_f) and the shape recovery ratio (R_r) were calculated based on the following formulas:

$$R_f = \frac{180^o - \theta_s}{180^o}$$

$$R_r = \frac{\theta_r}{180^o - \theta_s}$$

in the formulas above, θ_s is sagging angle when the external force is removed in the cold; θ_r is shape recovery angle in the shape recovery process.

3. Results and discussion

A double screw extruder with six temperature controllers was used to manufacture PLA filaments and PLA/Fe_3O_4 composite filaments, see Fig. 1(a). These shape memory filaments can be used to print complex structures by commercial FDM printers. SEM images of the cross-section of PLA/Fe_3O_4 composite filaments are shown in Fig. 1(b). From the SEM image we can see that Fe_3O_4 magnetic particles are distributed uniformly in the filaments. The printed structures with Fe_3O_4 particles can be triggered in magnetic field, causing the uniform heat. The printing process shown in Fig. 1(c), is controlled by the temperature of

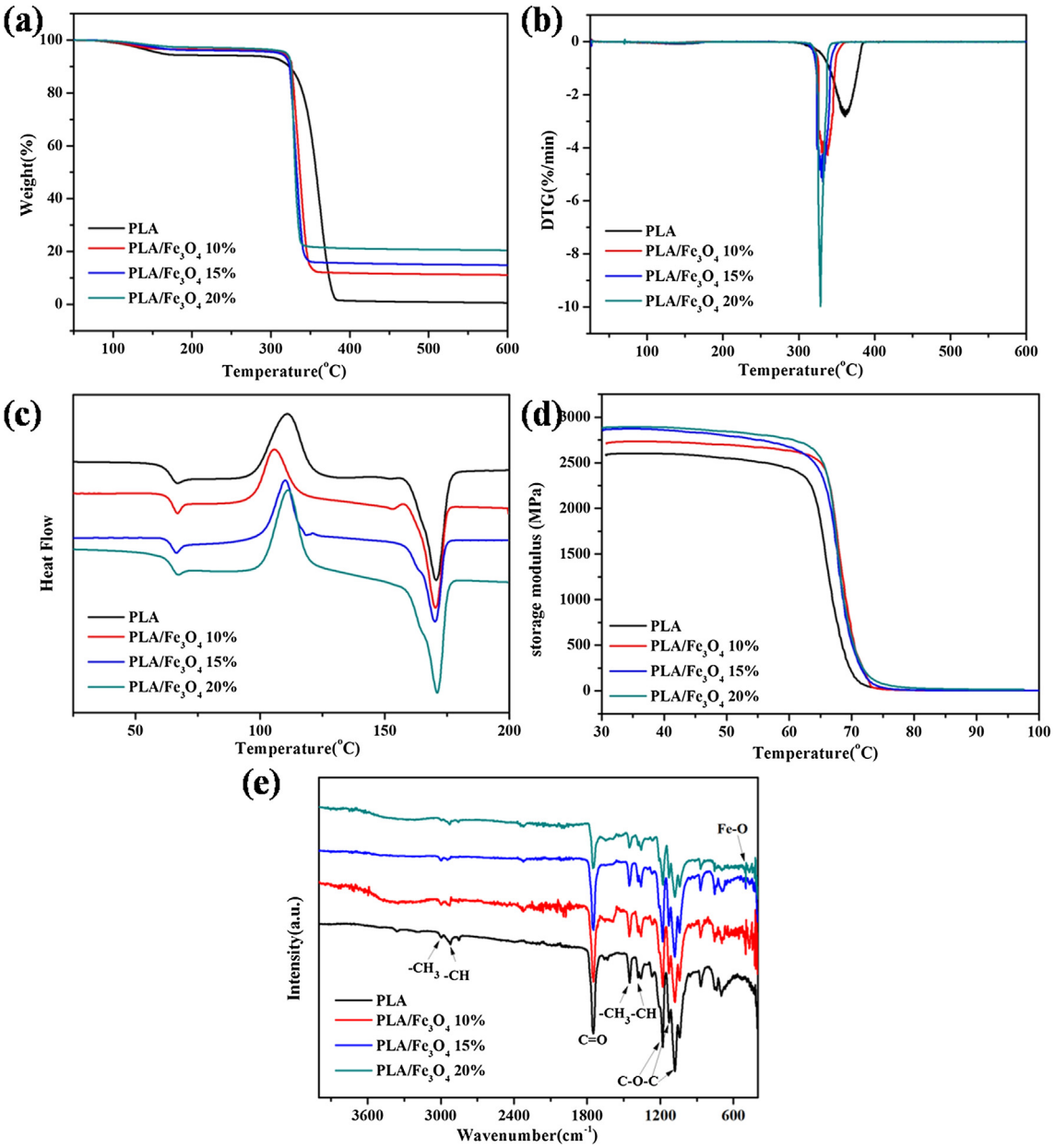

Fig. 2. PLA/Fe_3O_4 composite filaments with different contents of Fe_3O_4: (a) TGA curves, (b) DTG curves, (c) DSC curves, (d) DMA images and (e) FTIR.(For interpretation of the references to colour in this figure legend, the reader is referred to the web version of this article.)

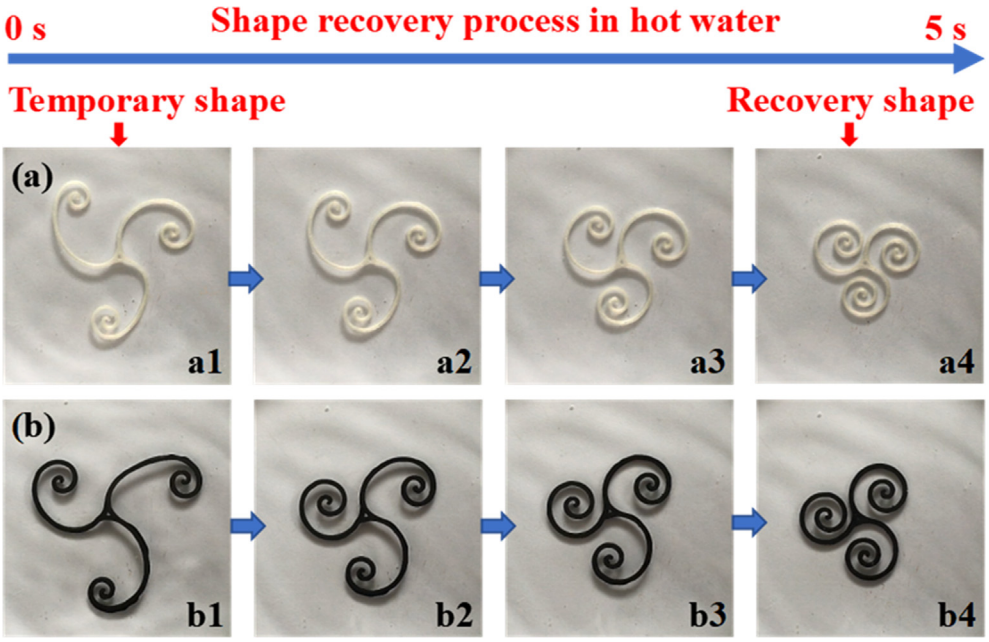

Fig. 3. Deployable behaviors of 4D printed structures in hot water: (a) PLA, (b) PLA/Fe_3O_4. (For interpretation of the references to colour in this figure legend, the reader is referred to the web version of this article.)

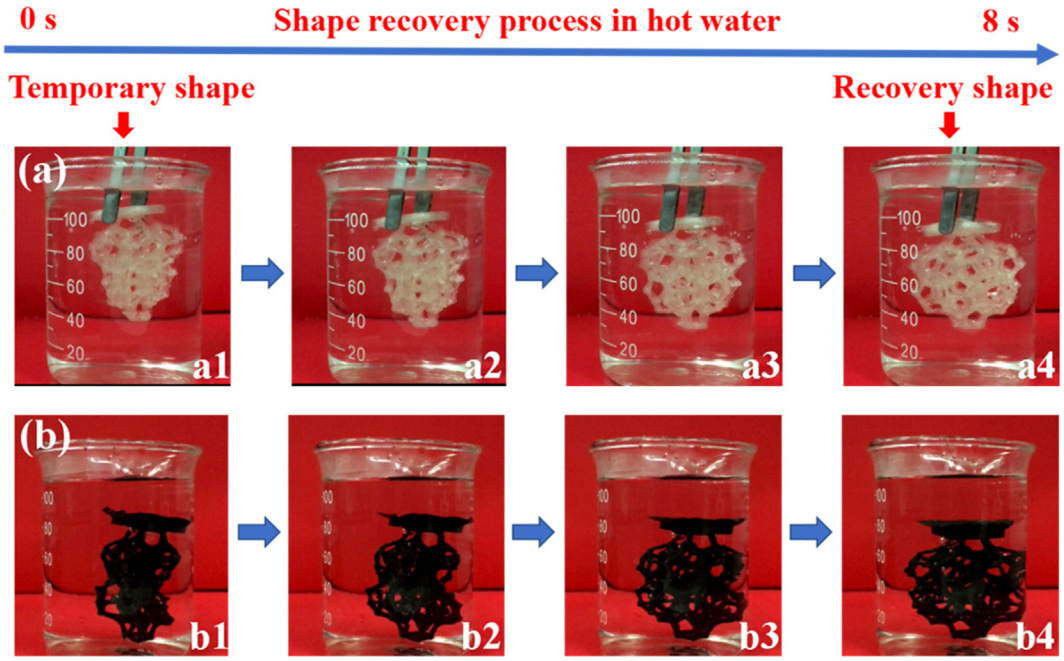

Fig. 4. Expansion behaviors of 4D printed complex structures in hot water: (a) PLA, (b) PLA/Fe_3O_4. (For interpretation of the references to colour in this figure legend, the reader is referred to the web version of this article.)

Table 2
Shape memory properties of PLA/Fe_3O_4 composites at T_{tran} +20 °C.

Sample\percent	PLA/Fe_3O_4 10%	PLA/Fe_3O_4 15%	PLA/Fe_3O_4 20%
Shape recovery ratio (R_r)	95.6%	95.8%	96.3%
Shape fixity ratio (R_f)	96.5%	96.9%	96.9%
Recovery time	5 s	5 s	5 s

the printing head and printing track to obtain the desired structure. Fig. 1(d) is the printed structure manufactured by PLA and PLA/Fe_3O_4 composite filaments. The samples with porous structures show potential applications in many fields, such as biomedical science.

The PLA/Fe_3O_4 composites with different contents of Fe_3O_4 magnetic particles were investigated. The TGA results illustrated that initial decomposition temperature of these composites with different contents of magnetic particles was more than 300 °C and final decomposition temperature was over 340 °C (Table 1). Initial decomposition temperature (T_d) is defined as the temperature of 5% weight loss and final decomposition temperature (T_{dmax}) is the temperature of no weight change. The TGA results in Fig. 2(a) illustrated that the initial decomposition temperatures of pure PLA and PLA composites with 10%, 15%, and 20% Fe_3O_4 particles are 161.54 °C, 314.42 °C, 311.84 °C and 302.35 °C, respectively. The final decomposition temperatures of the samples are 388.24 °C, 362.79 °C, 354.11 °C and 349.10 °C,

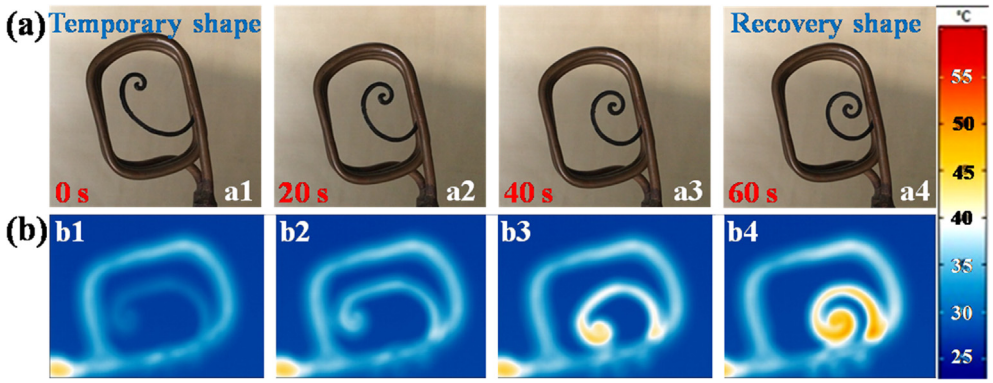

Fig. 5. Magnetic field triggered shape recovery behavior of 4D printed structures with 15% Fe_3O_4 at 27.5 kHz: (a) real process, (b) thermal distribution. (For interpretation of the references to colour in this figure legend, the reader is referred to the web version of this article.)

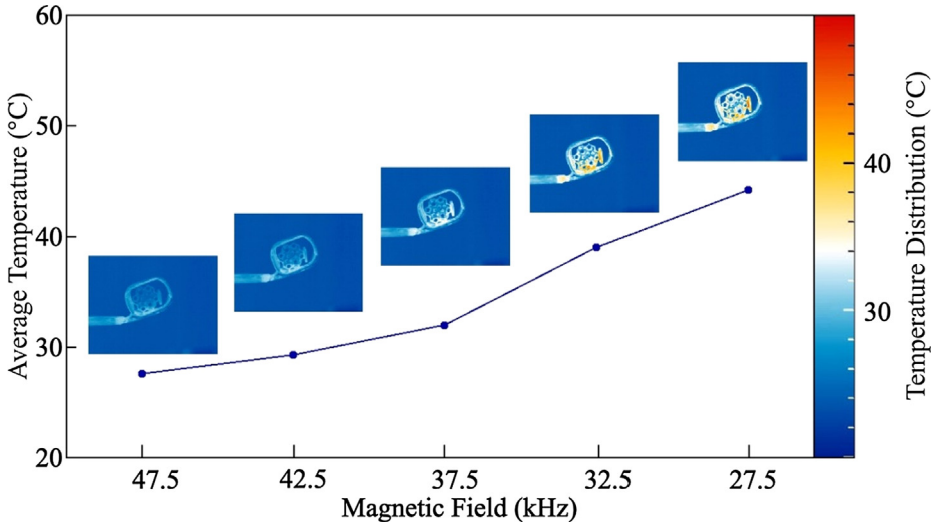

Fig. 6. Relationship between the average surface temperature and triggered frequency in magnetic field of 4D printed structure. (For interpretation of the references to colour in this figure legend, the reader is referred to the web version of this article.)

Table 3
Shape memory properties of PLA/Fe_3O_4 composites triggered by magnetic field.

Sample\percent	PLA/Fe_3O_4 10%	PLA/Fe_3O_4 15%	PLA/Fe_3O_4 20%
Shape recovery ratio (R_r)	95.5%	95.6%	96.3%
Shape fixity ratio (R_f)	96.6%	96.7%	96.8%
Recovery time	14 s	10 s	8 s
Frequency	27.5 kHz	27.5 kHz	27.5 kHz

respectively. The results show that the PLA composites with 10%, 15%, and 20% Fe_3O_4 particles have similar degradation temperatures. From DTG results in Fig. 2(b), we can know that decomposition rate increase with the increasing particle contents. The effects of the added Fe_3O_4 particles on the initial decomposition temperature and final decomposition temperature are contributed to the formation of Fe-O groups. Fig. 2(c) is the DSC curve of PLA/Fe_3O_4 composites, showing the transition temperatures of samples with 10%, 15%, and 20% Fe_3O_4 are respectively around 62.7 °C, 64.0 °C and 66.7 °C. As shown in Fig. 2(d), the storage modulus of the composites is more than 1600 MPa when the temperature is 40 °C. This means that the stiffness of the structure is maintained in the process of shape changing. The modulus of the composites decreases as a function of increasing temperature for all samples with different Fe_3O_4 concentrations. Fig. 2(e) shows the FTIR results of pure PLA and the composites with different contents of Fe_3O_4 particles. From the FTIR results we can see that there is no new peak with the change of Fe_3O_4 nanoparticle concentrations and the peak attributions were list as follows [38]. The peaks at 2980 cm^{-1} and 1500 cm^{-1} correspond to $-CH_3$ functional group. The IR peaks at 2950 cm^{-1} and 1400 cm^{-1} were attributed to −CH vibration. The peak at 1750 cm^{-1} reveals the stretching vibration of C═O group. C−O−C vibration was characterized at 1150 cm^{-1}, 1100 cm^{-1} and 1049 cm^{-1}, respectively. The peak near 500 cm^{-1} can be ascribed to Fe−O group. The transmittance and the relative intensity of peak decrease as the Fe_3O_4 concentration increases.

The shape memory performances of the 2D and 3D structures were investigated in hot water and the process included three steps: (1) The printed sample was deformed at 80 °C; (2) the deformed sample was cooled down at room temperature to obtain the temporary shape; (3) the deformed shape recover the original shape when heated to 80 °C again. As shown in Fig. 3(a) and (b), 4D printed flower structures by PLA and PLA/Fe_3O_4 filaments have a fast response speed and thus, both structures can recover the initial shape in hot water within 5 s. The printed structures consisting of PLA and PLA/Fe_3O_4 showed similar shape recovery process and speed.

Fig. 4(a) and (b) show the printed 3D bone structure based on PLA and PLA composite, respectively. The shape memory treatment process is similar to the 2D structures. The 4D printed bone structure can expand to the initial shape within 8 s. The shape recovering velocity was decreased by 3 s in comparison with the 2D structures because the 4D printed structures were larger with more structural details. The 4D structure made of PLA and PLA/Fe_3O_4 demonstrated similar shape recovery speed of 8 s in hot water.

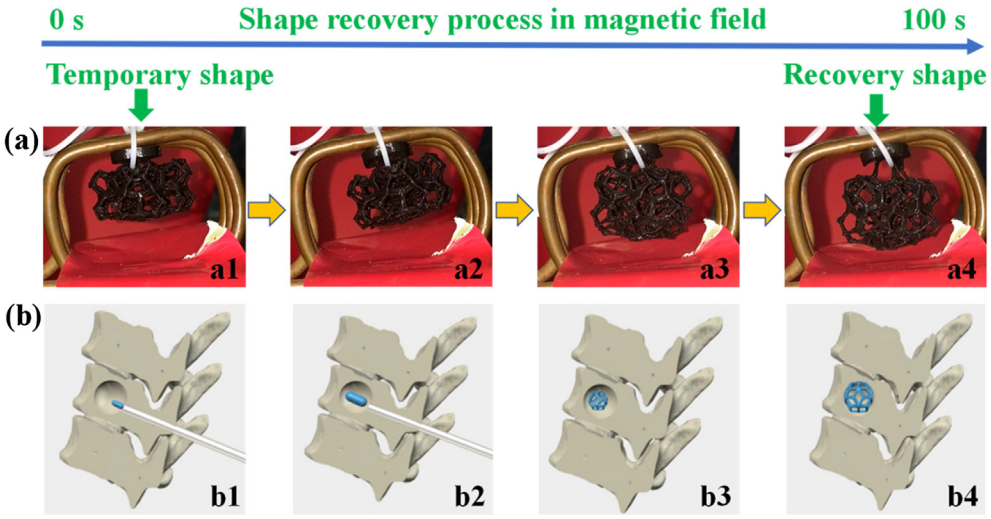

Fig. 7. (a) Shape recovery behavior of 4D printed composite structure in magnetic field, (b) A simulation showing the mechanism of the 4D structure as a bone repair tool. (For interpretation of the references to colour in this figure legend, the reader is referred to the web version of this article.)

The shape memory properties of PLA/Fe_3O_4 composite were calculated by formulas shown in experimental section. Table 2 indicates that the 4D printed structures with different amount of Fe_3O_4 shows similar shape recovery ratio, shape fixity ratio, and recovery time at a temperature which is 20 °C higher than glass transition temperature (T_{tran}). The printed structures were deformed to "U" shape for testing the shape memory performance. The shape recovery ratio and shape fixity were between 95.8% and 96.9%, respectively. In addition, the shape recover time was around 5 s.

Magnetic nanoparticles vibrate in an alternating magnetic field and generate heat. The heat generated provides the energy for shape changing. As shown in Fig. 5(a), the shape recovery behavior of the printed 2D PLA/Fe_3O_4 composite structure occurs when exposed to an alternating magnetic field at 27.5 kHz. The temporary shape returned to its initial shape after 60 s. Fig. 5(b) shows the recovery time and temperature distribution of the 4D printed structure with 15% Fe_3O_4 at 27.5 kHz. The temperature distribution was measured by infrared camera. The magnetic particles were uniformly distributed, inducing a uniform temperature change throughout the structure. The infrared thermograms demonstrated that the surface temperature of the 2D structure was around 40 °C which is close to human physiological temperature and within the temperature tolerance of the body, making it beneficial for the biomedical applications [33]. The reported work presented the same phenomenon [39].

The effect of magnetic field on the average surface temperature is also investigated, playing a significant role on shape memory performances of 4D printed structures. The 4D printed structure is triggered at different frequencies from 27.5 kHz to 47.5 kHz and the average surface temperature results are shown in Fig. 6. The surface temperature distribution of the printed complex structure in the magnetic field is uniform. With the frequency decreasing, the surface temperature increases from 20 °C to 40 °C, indicating that the material and structure design is suitable for tissue engineering.

Table 3 demonstrates that the shape recovery ratio and shape fixity of different 4D printed structures are comparable at around 95.5% and 96.7%. The recovery time reduced from 14 s to 8 s as the Fe_3O_4 concentration increased from 10% to 20% under the same magnetic field. The result indicated that the higher Fe_3O_4 concentrations can enable greater magnetite shape recovery force.

Fig. 7(a) demonstrates the shape recovery behavior of 4D printed structures in the shape of spinal bone. The bone structure can recover its initial shape within 100 s under a magnetic field, indicating the applicability of the 4D structure for personalized bone repair as different bone sizes can be custom-printed as required to fit the bone defect. A simulation showing the mechanism of the 4D structure as a bone repair tool is illustrated in Fig. 7(b). Here, we envisage that the bone structure is first compressed into a smaller size with memory of its original, large size. It can then be injected into the implant site. The compress structure can expand to the required shape and size in situ upon remote actuation by a magnetic field. Hence, the 4D printed PLA/Fe_3O_4 composite structure has great potential in biomedical applications, including but not limited to the bone tissue engineering example illustrated in this work [27,33].

4. Conclusions

In summary, we have demonstrated the shape memory capability of a range of 4D printed PLA/Fe_3O_4 composite structures. The mechanic and thermodynamic properties were analyzed. The shape recovery process under a specific temperature and magnetic field was characterized. The results indicated that the 4D printed complex structures have great potential functionality in biological and medical applications, including but not limited to bone tissue repair.

Declaration of Competing Interest

Authors declare that there are no conflict of interest.

Acknowledgments

This work is funded by the National Natural Science Foundation of China (Grant Nos. 11632005, 11672086, 11802075) and the Foundation for Innovative Research Groups of the National Natural Science Foundation of China (Grant No. 11421091). This work was also supported by the China Postdoctoral Science Foundation funded project.

References

[1] Momeni F, Mehdi Hassani SM, Liu NX, Ni J. A review of 4D printing. Mater Des 2017;122:42–79.
[2] Ding Z, Yuan C, Peng X, Wang TJ, Qi HJ, Dunn ML. Direct 4D printing via active composite materials. Sci Adv 2017:3e1602890.
[3] Wu JJ, Huang LM, Zhao Q, Xie T. 4D Printing: history and recent progress. Chin J Polym Sci 2018;36:563–75.
[4] Akbari S, Sakhaei AH, Kowsari K, Serjouei A, Zhang YF, Ge Q. Enhanced multi-material 4D printing with active hinges. Smart Mater Struct 2018;27:065027.
[5] Zarek M, Layani M, Cooperstein I, Sachyani E, Cohn D, Magdassi S. 3D printing of

shape memory polymers for flexible electronic devices. Adv Mater 2016;28:4449–54.
[6] Yang H, Leow WR, Wang T, Wang J, Yu JC, He K, et al. 3D printed photoresponsive devices based on shape memory composites. Adv Mater 2017;29:1701627.
[7] Zarek M, Mansour N, Shapira S, Cohn D. 4D printing of shape memory-based personalized endoluminal medical devices. Macromol Rapid Comm 2017;38:1600628.
[8] Miao S, Castro N, Nowicki M, Xia L, Cui H, Zhou X, et al. 4D printing of polymeric materials for tissue and organ regeneration. Mater Today 2017;20:577–91.
[9] Han YT, Hu JL, Jiang L. Collagen skin, a water-sensitive shape memory material. J Mater Chem B 2018;6:5144–52.
[10] Guo Y, Lv Z, Huo Y, Sun L, Chen S, Liu Z, et al. Biodegradable functional water-responsive shape memory polymer for biomedical applications. J Mater Chem B 2019;7:123–32.
[11] Quan Z, Wu A, Keefe M, Qin X, Yu J, Suhr J, et al. Additive manufacturing of multi-directional preforms for composites: opportunities and challenges. Mater Today 2015;18:503–12.
[12] Choi J, Kwon OC, Jo W, Lee HJ, Moon MW. 4D printing technology: a review. 3D Print. Addit Manuf 2015;2:159–67.
[13] Gladman AS, Matsumoto EA, Nuzzo RG, Mahadevan L, Lewis JA. Biomimetic 4D printing. Nat Mater 2016;15:413–8.
[14] Ge Q, Sakhaei AH, Lee H, Dunn CK, Fang NX, Dunn ML. Multimaterial 4D printing with tailorable shape memory polymers. Sci Rep 2016;6:31110.
[15] Caputo MP, Berkowitz AE, Armstrong A, Müllner P, Solomon CV. 4D printing of net shape parts made from Ni-Mn-Ga magnetic shape-memory alloys. Addit Manuf 2018;21:579–88.
[16] Kirillova A, Maxson R, Stoychev G, Gomillion CT, Ionov L. 4D biofabrication using shape-morphing hydrogels. Adv Mater 2017:291703443.
[17] Ambulo CP, Burroughs JJ, Boothby JM, Kim H, Shankar MR, Ware TH. Four-dimensional printing of liquid crystal elastomers. ACS Appl Mater Interf 2017;9:37332–9.
[18] Behl M, Lendlein A. Shape-memory polymers. Mater Today 2007;10:20–8.
[19] Leng JS, Lan X, Liu YJ, Du SY. Shape-memory polymers and their composites: stimulus methods and applications. Prog Mater Sci 2011;56:1077–135.
[20] Hu JL, Zhu Y, Huang HH, Lu J. Recent advances in shape-memory polymers: structure, mechanism, functionality, modeling and applications. Prog Polym Sci 2012;37:1720–63.
[21] Hardy JG, Palma M, Wind SJ, Biggs MJ. Responsive biomaterials: advances in materials based on shape-memory polymers. Adv Mater 2016:285717–24.
[22] Tibbits S. The emergence of “4D printing”. TED Talk 2013.
[23] Zhong XK, Joanne EMT, Liu Y, Chua CK, Yang SF, An J, et al. 3D printing of smart materials: a review on recent progresses in 4D printing. Virt Phys Prototyp 2015;10:103–22.
[24] Li X, Shang JZ, Wang Z. Intelligent materials: a review of applications in 4D printing. Assemb Automat 2017;2:170–85.
[25] Bodaghi M, Damanpack AR, Liao WH. Triple shape memory polymers by 4D printing. Smart Mater Struct 2018;27:065010.
[26] Ge Q, Dunn CK, Qi HJ, Dunn ML. Active origami by 4D printing. Smart Mater Struct 2014;23:094007.
[27] Huang LM, Jiang RQ, Wu JJ, Song JZ, Bai H, Li BG, et al. Ultrafast digital printing toward 4D shapechanging materials. Adv Mater 2017;29:1605390.
[28] Wei HQ, Zhang QW, Yao YT, Liu LW, Liu YJ, Leng JS. Direct-write fabrication of 4D active shape-changing structures based on a shape memory polymer and its nanocomposite. ACS Appl Mater Interf 2017;9:876–83.
[29] Zhang W, Zhang FH, Lan X, Leng JS, Wu AS, Bryson TM, et al. Shape memory behavior and recovery force of 4D printed textile functional composites. Compos Sci Technol 2018;160:224–30.
[30] Liu Y, Zhang W, Zhang FH, Lan X, Leng JS, Liu S, et al. Shape memory behavior and recovery force of 4D printed laminated Miura-origami structures subjected to compressive loading. Compos B 2018;153:233–42.
[31] Li YC, Zhang YS, Akpek A, Shin ST, Khademhosseini A. 4D bioprinting: the next-generation technology for biofabrication enabled by stimuli-responsive materials. Biofabriction 2017;9:012001.
[32] Hendrikson WJ, Rouwkema J, Clementi F, Blitterswijk CA, Fare S, Moroni L. Towards 4D printed scaffolds for tissue engineering: exploiting 3D shape memory polymers to deliver time-controlled stimulus on cultured cells. Biofabrication 2017;9:031001.
[33] Senatov FS, Niaza KV, Zadorozhnyy MY, Maksimkin AV, Kaloshkin SD, Estrin YZ. Mechanical properties and shape memory effect of 3D-printed PLA-based porous scaffolds. J Mech Behav Biomed Mater 2016;57:139–48.
[34] Miao SD, Zhu W, Castro NJ, Nowicki M, Zhou X, Cui HT, et al. 4D printing smart biomedical scaffolds with novel soybean oil epoxidized acrylate. Sci Rep 2016;6:27226.
[35] Stoychev G, Puretskiy N, Ionov L. Self-folding all-polymer thermoresponsive microcapsules. Soft Matt 2011;7:3277–9.
[36] Senatov FS, Zadorozhnyy MY, Niaza KV, Medvedev VV, Kaloshkin SD, Anisimova NY, et al. Shape memory effect in 3D-printedscaffolds for self-fitting implants. Eur Polym J 2017;93:222–31.
[37] Cabrera MS, Sanders B, Goor O, Driessen-Mol A, Oomens C, Baaijens F. Computationally designed 3D printed self-expandable polymerstents with biodegradation capacity for minimally invasive heart valve implantation: a proof-of-concept study. 3D Print Addit Manuf 2017;4:19–29.
[38] Chen F, Gao Q, Hong G. Synthesis of magnetite core-shell nanoparticles by surface-initiated ring-opening polymerization of L-lactide. J Magn Magn Mater 2008;320:1921–7.
[39] Zhang FH, Zhang ZC, Luo CJ, Lin IT, Liu YJ, Leng JS, et al. Remote, fast actuation of programmable multiple shape memory composite by magnetic fields. J Mater Chem C 2015;3:11290–3.